4- THE IMPRINT OF SEDIMENT-DERIVED FLUIDS ON MELTING OF MORB AMPHIBOLITE IN A SUBDUCTION SETTING (SIERRA DEL CONVENTO MÉLANGE, CUBA)

C. Lázaro[(1)], I.F. Blanco-Quintero[(1)], C. Marchesi[(2)], D. Bosch[(2)], A. García-Casco[(1,3)]

(1) Departamento de Mineralogía y Petrología, Universidad de Granada, Avda. Fuentenueva s/n, 18002 Granada, Spain.

(2) Geosciences Montpellier, Equipe Manteau-Noyau, UMR 5243, CNRS-Universite Montpellier II, 34095, Montpellier, France.

(3) Instituto Andaluz de Ciencias de la Tierra, CSIC-Universidad de Granada, Avda. Fuentenueva s/n, 18002 Granada, Spain.

ABSTRACT

Major and trace element geochemical signatures and Sr–Nd isotope data of muscovite (Ms)-bearing amphibolite blocks and associated muscovite-bearing trondhjemitic and quartz-muscovite rocks from the Sierra del Convento mélange (eastern Cuba) indicate that oceanic crust underwent partial melting processes during subduction and accretion to the upper plate triggered by the infiltration of fluids evolved from the subducting sediments. REE patterns of the Ms-trondhjemites are fractionated ($2<(La/Yb)n<62$), with LREE enrichment and HREE depletion. These patterns are similar to adakitic melts formed by partial melting of mafic material at moderate to high pressure. Indeed, Ms-trondhjemites from Sierra del Convento mélange exhibit geochemical features considered distinctive of adakites, including SiO_2>56 wt %, high Na_2O contents (4.5-9 wt.%), (K_2O/Na_2O)≈0.42, Mg#≈50, LREE enrichment, HREE depletion, and high La/Yb and Sr/Y. We consider that these rocks represent an end-member of the volcanic arcs series formed at depth in the subduction environment that did not react with the mantle wedge before eruption. Furthermore, we have identified the crystallization products (Qtz-Ms rocks, highly enriched in LILE, K and Ba) of the primary fluids evolved from subducted sediments that infiltrated the accreted blocks of MORB amphibolite and promoted their partial melting under water-saturated conditions.

Keywords: Slab melt, Adakite, Fluid composition, sedimentary imprint, Sr–Nd isotopes

INTRODUCTION

Different conditions may trigger partial melting of the slab and/or the overlying mantle wedge in subduction settings. In cold subduction zones the geothermal conditions of the slab may not allow attaining P–T conditions for melting at sub-arc depths (ca. 150 km), but triggers dehydration of the slab and the release of large ion lithophile element (LILE)-enriched hydrous fluids that metasomatize the overlying mantle wedge and instigate its melting (e.g. Gill,1981; Kushiro,1990; Tatsumi and Kogiso, 1997). Partial melting of the slab is however inferred to occur at sub-arc depths in many warm and hot subduction zones (Bebout, 2007). These melts may eventually reach shallow depths in the volcanic arc after infiltration through the mantle wedge (and triggering its melting, Rapp et al., 1999) or after formation of underplated mantle wedge plumes (Gerya and Yuen, 2003; Gorczyk et al., 2007; Castro and Gerya, 2008; Castro et al., 2010). However, direct observation of processes taking place at sub-arc depths is hampered by the scarcity of rocks that escaped burial into the mantle.

Examples of pristine slab-derived melts that reached the Earth's surface are scarce. Only in rare cases of oceanic subduction complexes, such as the Catalina Schist mélange (California) and the Sierra del Convento and La Corea mélanges (eastern Cuba), partial melting of metabasite and metasomatic mass-transfer processes in the slab have been described (Sorensen, 1988; Sorensen and Grossman, 1989; Bebout and Barton, 1993; Grove and Bebout, 1995; García-Casco, 2007; García-Casco et al., 2008a; Lázaro and García-Casco, 2008; Blanco-Quintero et al., 2010a). The tonalitic–trondhjemitic rocks produced after melting of amphibolite in the Catalina Schist were considered as primary adakitic liquids by Martin (1999). The geochemical characteristics of K-poor tonalitic-trondhjemitic rocks of the Sierra del Convento mélange indicate that they constitute pristine partial melts formed after fluid-fluxed melting of subducted N-MORB garnet-epidote amphibolite in response to a very hot subduction scenario likely caused by subduction of a young hot slab (García-Casco et al,. 2008a; Lázaro and García-Casco, 2008). The depth of melting was ca. 50 km, shallower than typical sub-arc depths where slab melts segregate from garnet+clinopyroxene-rich residues. Elemental and isotopic features of the K-poor tonalitic-trondhjemitic rocks of the Sierra del Convento exclude a sediment source for the infiltrating fluid and suggest, in turn a fluid evolved from a depleted source such as dehydrating serpentinite from the downgoing slab (Lázaro and García-Casco, 2008).

Recently, however, we have identified K-rich trondhjemitic rocks in the Sierra del Convento and La Corea mélanges (eastern Cuba). These rocks formed after partial melting of MORB-derived amphibolite and crystallized at depth in the subduction environment, same as the K-poor trondhjemites described so far (references above), but are strongly enriched in LIL elements such as K, Ba, Rb, suggesting a different source for the infiltrating fluid. In this paper, we characterize the major, trace element and Sr–Nd isotope geochemistry of K-rich primary melts, residual rocks, and hydrothermal rocks produced in the hot subduction scenario of the Sierra del Convento mélange.

GEOLOGICAL SETTING

The Greater Antilles constitute an orogenic belt located at the northern margin of the Caribbean plate that documents the collision of a Mesozoic–Tertiary volcanic arc with buoyant parts of the North American plate during the Late Mesozoic and Tertiary. The orogenic belt is mainly composed of oceanic material, including ophiolites and intra-oceanic volcanic arc complexes, as well as continental material represented by fragments of the southern borderlands of North America (Bahamas platform and the Maya block) and the Caribeana terrane (García-Casco et al., 2008b). All these terrains are well exposed in Cuba (Fig. 1a), where the oceanic material includes the northern and eastern ophiolite belts and the Cretaceous and Palaeogene volcanic arcs (Iturralde-Vinent, 1998 and references therein).

In eastern Cuba, the ophiolitic belt is formed by two large bodies named Mayarí-Cristal and Moa-Baracoa. The elemental and isotopic composition of these complexes indicates a supra-subduction environment (Marchesi et al., 2006, 2007; Proenza et al., 2006). The ophiolitic bodies form the highest structural complexes in the region, overriding the volcanic-arc complexes. The latter, formed by the Santo Domingo (to the NW) and the Purial (tom the S-SE) complexes, have been classically considered the eastern continuation of the western and central Cuban Cretaceous volcanic arc complex (Fig. 2a; Iturralde-Vinent et al., 1996, 2006). They are composed of tholeiitic and calcalkaline volcanic arc sequences (Gyarmati et al., 1997), and the Purial complex was metamorphosed to greenschist and blueschist facies (Boiteau et al., 1972; Somin and Millán, 1981; Cobiella et al., 1984; Millán and Somin, 1985; Millán, 1996) during latest Cretaceous (70-75 Ma) times (Somin et al., 1992; Iturralde-Vinent et al., 2006).

Mélange complexes made of serpentinitic matrix enclosing high pressure metamorphic exotic blocks crop out below the ophiolitic bodies and above the volcanic arc complexes The most significant serpentinite mélanges are the Sierra del Convento and La Corea mélanges, both sharing similar lithological assemblages (Somin and Millán, 1981; Kulachkov and Leyva, 1990; Hernández and Canedo, 1995; Leyva, 1996; Millán, 1996; Blanco-Quintero, 2003; García-Casco et al., 2006, 2008a). The Sierra del Convento mélange, located in the south, overrides the Purial complex (Fig. 1a,b). The La Corea mélange is located in the Sierra de Cristal, and is associated with the Mayarí-Cristal ophiolitic body (Fig. 1a). The serpentinitic matrix is made of antigoritite and formed deep in the subduction environment after hydration of upper plate harzburgitic rocks (Blanco-Quintero et al., 2010b). These mélanges have been interpreted as fragments of the subduction channel related to south-westward-directed subduction on the leading edge of the Caribbean plate during the Cretaceous (García-Casco et al., 2006, 2008a,b; Blanco-Quintero et al., 2010a, b).

The main type of block in these melanges is epidote ± garnet amphibolite and associated leucocratic trondhjemite-tonalite rocks. The amphibolites show variable grain size and extent of deformation and recrystallization (García-Casco et al, 2008a). They are foliated and mainly composed of amphibole+epidote±quartz±garnet and have major and trace element geochemistry indicative of N-MORB signature (Lázaro and García-Casco, 2008). Leucocratic rocks of trondhjemitic–tonalitic composition are commonly associated with the amphibolites and constitute their partial melting product at 700-750 ºC ca. 15 kbar

(García-Casco et al, 2008a; Lázaro and García-Casco, 2008; Blanco-Quintero et al., 2010a). They are formed by primary (magmatic) plagioclase+quartz+epidote±paragonite±pargasite, have variable grain size, and show minor deformation.

Muscovite-bearing amphibolites and trondhjemites constitute rock varieties associated with Ms-lacking lithologies. This paper examines the geochemistry of these muscovite-bearing rocks in order to get insight into the source and role of slab-derived fluids in the generation of slab magmas. The rocks examined are muscovite-bearing amphibolites (samples CV139a, CV140a, CV230a, CV230c), trondhjemites (SC-20, CV230e, CU-72-I, CU-72), locally with pegmatitic texture (CV201a, CV201g, CV201h), and Qtz-Ms hydrothermal rocks (CV201d, CV201f, CV53e-I, CV53e-II) that crosscut other types of rock or form discrete bodies.

ANALYTICAL TECHNIQUES

Bulk-rock chemistry

Powered whole-rock samples were obtained by grinding in a tungsten carbide mill. Major element and Zr compositions were determined on glass beads, made of 0.6 g of powered sample diluted in 6 g of $Li_2B_4O_7$, by a PHILIPS Magix Pro (PW-2440)

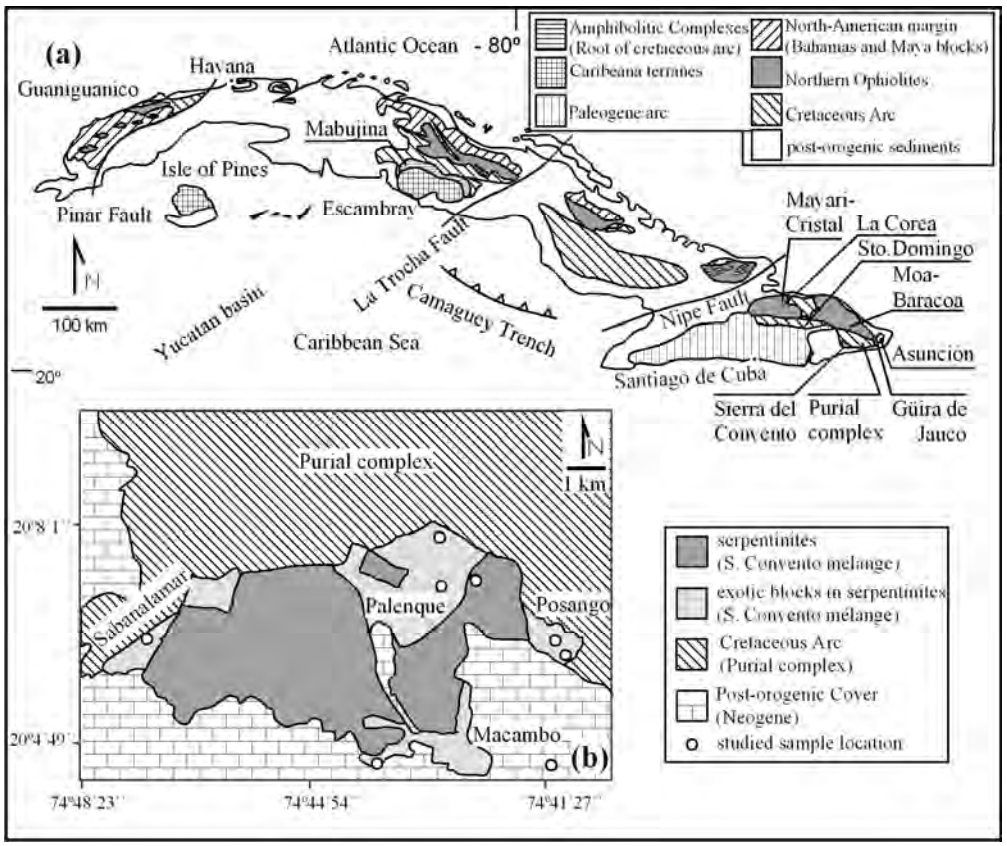

Fig. 1. (a) General geological map of Cuba (Iturralde-Vinent, 1998) showing the main geological units, (b) Geological map of Sierra del Convento (Kulachkov and Leyva, 1990) with location of sample sites.

X-ray fluorescence (XRF) equipment at the University of Granada (Centro de Instrumentación Científica, CIC). Precision was better than ±1.5% for an analyte concentration of 10 wt.%. Precision for Zr and LOI is better than ±4% at 100 ppm concentration. The analyses were recalculated to an anhydrous 100 wt % basis compositions, and these new data are used in the text and figures. The Mg number (Mg#) is expressed (100*molar MgO/(MgO+FeOtot)).

Trace element, except Zr, were determined at the University of Granada (CIC) by ICP-Mass Spectrometry (ICP-MS) after HNO_3+HF digestion of 0.1000 g of sample powder in a Teflon-lined vessel at ~180 °C and ~200 p.s.i. for 30 min, evaporation to dryness, and subsequent dissolution in 100 ml of 4 vol % HNO_3. Blanks and international standards PMS, WSE, UBN, BEN, BR, and AGV (Govindaraju, 1994) were run as unknowns during analytical sessions. Precision was better than ±2% and ±5% for analyte concentrations of 50 and 5 ppm.

Isotope analysis

Isotope analyses were carried out at the University of Granada (CIC). Whole rock samples for Sr and Nd isotope analyses were digested in the same way as for ICP-MS analysis, using ultra-clean reagents and analyzed by thermal ionization mass spectrometry (TIMS) in a Finnigan Mat 262 spectrometer after chromatographic separation with ion exchange resins. Normalization values were 86Sr/88Sr=0.1194 and 146Nd/144Nd=0.7219. Blanks were 0.6 and 0.09 ng for Sr and Nd, respectively. The external precision (2σ), estimated by analysing 10 replicates of the standard WSE (Govindaraju, 1994), was better than 0.003% for $^{87}Sr/^{86}Sr$ and 0.0015% for $^{143}Nd/^{144}Nd$. The $^{87}Sr/^{86}Sr$ measured value in the laboratory for NBS 987 international standard was 0.710250±0.0000044 (2σ, n=106). Measurements of La Jolla Nd international standard on this mass spectrometer yield a $^{143}Nd/^{144}Nd$ ratio of 0.511844±0.0000067 (2σ, n=49).

PETROGRAPHY

Peak metamorphic mineral assemblage of the studied Ms-amphibolite samples consists of pargasitic amphibole, epidote, garnet, phengite, rutile, titanite, and accessory apatite and quartz (Fig. 2a; Table 1). These assemblages define a crude foliation mainly marked by phengite and pargasite crystals. Quartz appears as small dispersed grains in the matrix, but quartz-absent samples are common. Garnet has been observed in all the studied samples (Table 2). It forms large porphyroblasts containing inclusions of amphibole and epidote (Fig. 2a). Phengitic mica appears as idiomorphic and medium grained crystals. Titanite forms idiomorphic crystals elongated along the foliation, but it also replaces rutile. Retrograde overprints consist of association of glaucophane, actinolite, (clino)zoisite, chlorite, pumpellyite, and, less abundantly, albite and paragonite. All these retrograde minerals are fine-grained and corrode the peak-metamorphic minerals, but they are also dispersed in the matrix or located in fractures. Retrograde glaucophane is typically aggregated with actinolite, chlorite and albite, and commonly overprints peak amphibole (Fig. 2a). Chlorite and pumpellyite replace garnet and pargasite. Retrograded crystals of pargasite commonly contain small needles of exsolved rutile or titanite.

The magmatic mineral assemblage of the Ms-trondhjemites (including the pegmatitic varieties) is composed of medium-grained plagioclase, quartz and phengite, with subordinate epidote, plus accessory apatite, titanite, and rutile (Fig. 2b; Table 2). Garnet is occasionally present. Epidote and garnet are idiomorphic and medium grained. Phengite is idiomorphic and has medium grain size. Retrograde mineral assemblages overprint the magmatic assemblages. Magmatic plagioclase appears generally transformed to retrograde albite plus fine-grained (clino)zoisite, paragonite, phengite, and, locally, lawsonite. Magmatic epidote is overprinted by fine grained overgrowths of (clino)zoisite. Glaucophane is absent. Titanite replaces rutile. Very small amounts of retrograde K-feldspar, celsian and cymrite have been observed in some samples.

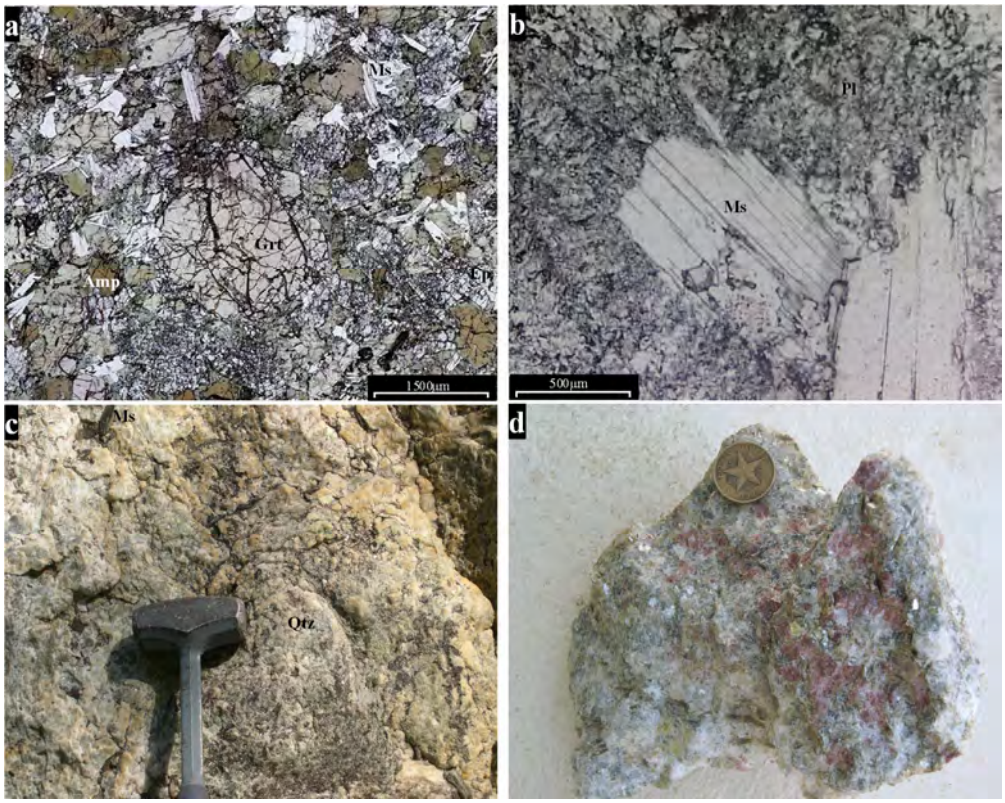

Fig. 2. (a) Photomicrograph of Ms-amphibolite composed of amphibole, epidote, garnet, mica (phengite) and titanite. (b) Photomicrograph of a Ms-trondhjemite bearing plagioclase, muscovite, quartz and clinozoisite-epidote. (c) Qtz-Ms block. (d) Garnet-bearing Qtz-Ms rock. The scale bar is 1500 µm in (a) and 500 µm in (b). Mineral abbreviations after Kretz (1983).

Table 1 Mineral abundance in the studied samples (visual estimates).

	peak metamorphic / magmatic										retrograde									
	Amp	Ep	Grt	Phe	Qtz	Pl	Pa	Rt	Ttn	Ap	CaAmp	Gl	Chl	Pmp	Ab	Lws	Pa	Czo	Kfs
Ms-amphibolites																				
CV139a	45	20	20	10	5				x			x	x	x	x	x				
CV140a	55	15	10	15	5			x				x	x	x	x					
CV230c	74	10	10	5					1			x	x	x	x			x	x	
CV230a	55	25	15						5			x	x	x	x				x	
Ms-trondhjemites																				
CV201a	x		20	30	40				x				x			x		10	x	
CV201g		x	20	20	50														x	
SC-20	8	x	x	20	55	x							x			3	10	4		
CV201h			20	15	55										x	1	4	5		
CV230e			5	35	55													5	x	
CU-72-I		2	10	30	45								x			5	x	3		
CU-72		1	10	30	45								x			5	x	4		
Qtz-Ms rocks																				
CV201d			55	45	x														x	
CV201f			35	65															x	
CV278a-I			10	35	55														x	
CV53e-I			45	55																
CV53e-II			45	55																

The Qtz-Ms rocks present a mineralogy essentially composed of medium to coarse size crystals of quartz and phengite (Fig. 2c). Sample CV278a-I also has coarse garnet crystals (Fig. 2d). Scarce fine-grained of K-feldspar is also present in all the samples.

GEOCHEMISTRY

Major elements

Ms-amphibolites

The SiO_2 contents of Ms- bearing amphibolite range from 42.1 to 46.5 wt % (Table 2), varying from picro-basaltic to basaltic compositions in the TAS diagram (Le Maitre et al., 1989), lying on the sub-alkaline-alkaline field (Fig. 3a). They have medium-K to high-K calc-alkaline affinity in the SiO_2-K_2O diagram (Fig. 3b; Peccerillo and Taylor, 1976) but, as discussed below, K_2O (and Na_2O) contents do not represent primary (magmatic) abundances. In general, the samples have higher contents in K_2O (Fig. 3b), Al_2O_3, and BaO, and significantly lower contents in MgO (Fig. 4) than the Ms-lacking amphibolites of Sierra del Convento mélange (Lázaro and García-Casco, 2008).

Notably, the samples show quite variable Na_2O contents (1.17-4.17 wt %), so that two samples have high inverse agpaitic index as compared to MORB and other amphibolites from the Sierra del Convento while another two samples present a similar inverse agpaitc index as MORB (Fig. 5).

Ms-trondhjemites

Ms-trondhjemites in the TAS diagram have rhyolite composition, except one sample which has trachyte composition (Fig. 3a), with SiO_2 contents ranging from 65.6 to 75.6 wt %. They have low-K tholeiitic to medium-K calc-alkaline affinity (Fig. 3b). They have Na_2O and K_2O contents ranging from 5.4 to 9 wt % and from 0.77 to 1.74 wt %, respectively. The Mg# values, from 14 to 60, are lower than or similar to those of Ms-lacking trondhjemites (Fig. 4).

Considering amphibolites and trondhjemites in Harker diagrams, they show similar trends to those of Ms-lacking amphibolite-trondhjemite rocks (Lázaro and García-Casco, 2008) and acid rocks from the Catalina Schist (Fig. 4), except for higher SiO_2, K_2O and BaO contents (Fig. 3b and Fig. 4). A gap in silica content ranging from 47 to 66 wt.% SiO2 is consistent with derivation of the trondhjemitic rocks from partial melting of amphibolites and melt extraction (cf., Lázaro and García-Casco, 2008).

Importantly, the Ms-trondhjemites are Al-saturated (i.e. peraluminous; ASI = 1.108-1.289; Fig. 5) and plot close to the alkali feldspar-white mica mixing line delineated in Fig. 5. In the CIPW normative An-Ab-Or diagram of O´Connor (1965), with the classification of acid and intermediate rocks modified by Barker (1979), these samples mainly plot in the trondhjemitic field (Fig. 6).

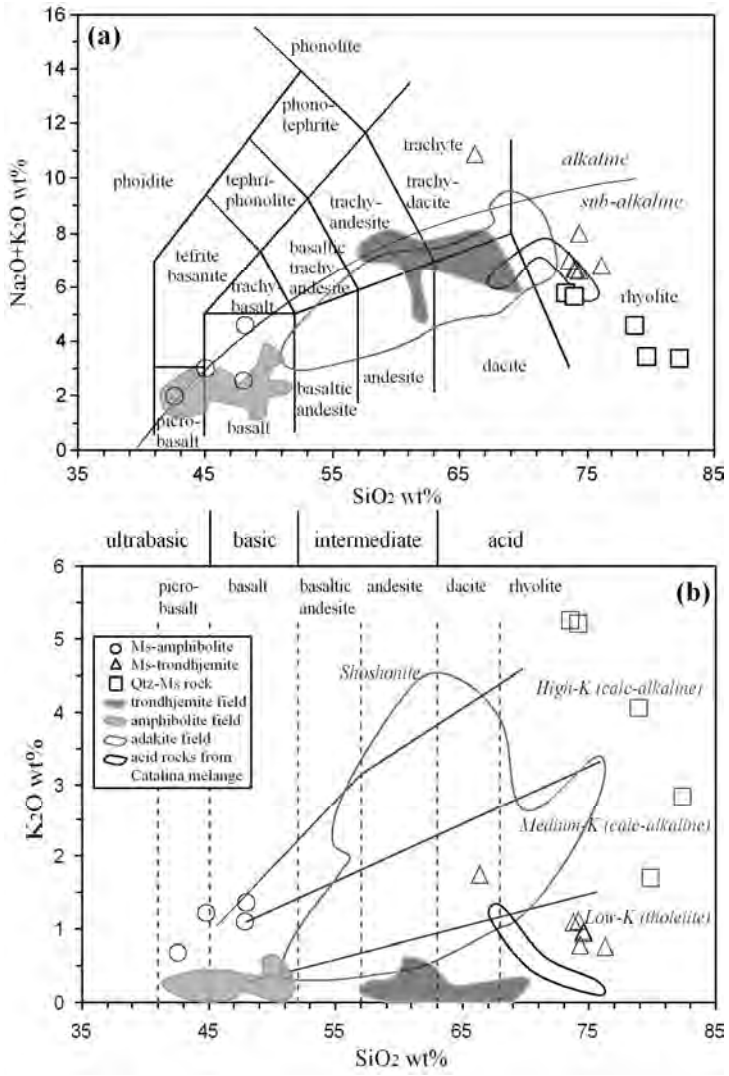

Fig. 3. (a) TAS diagram of classification of volcanic rocks from Le Maitre et al. (1989) and (b) K_2O vs. SiO_2 diagram (Peccerillo and Taylor, 1976) with subdivision of volcanic series and TAS based names of rocks of the subalkaline series. The diagrams contain the studied Ms-amphibolites, Ms-trondhjemites, Qtz-Ms rocks and, for comparison, the K-poor amphibolites and trondhemites from the Sierra del Convento mélange (Lázaro and García-Casco, 2008), acid rocks from the Catalina mélange, California (pegmatites and leucocratic segregates, Sorensen and Grossman, 1989); Cenozoic adakites from the Aleutians (Yogodzinski et al., 1995), Argentina (Benoit et al., 2002), Chile (Stern and Kilian, 1996), Ecuador (Beate et al., 2001; Bourdon et al., 2002; 2003; Samaniego et al., 2005), Philippines (Sajona et al., 1996; 2000), Japan (Morris, 1995), Panama-Costa Rica (Defant et al., 1992), USA (Smith and Leeman, 1987); and average adakite values (Martin, 1999; Smithies, 2000). All analyses normalized to 100 wt% anhydrous.

Qtz-Ms rocks

Qtz-Ms rocks are hydrothermal and are not suitable of classification in geochemical diagrams devised for igneous rocks. However, for comparison, they have been plotted in the same diagrams. Their SiO_2 contents range from 71.5 to 81.2 wt % (Fig. 3). Contents of K_2O are higher than 1.7 wt %, reaching 5.1 wt %. These rocks

have lower Na_2O contents (<1.66 wt %) than the Ms-trondhjemites, while the Al_2O_3 contents are similar (12.3-18.3 wt %). They are depleted in CaO, with contents lower than 0.2 wt %. These Qtz-Ms veins show significant contents in BaO, reaching values of 1.35 wt % (Fig. 4).

Similar to the Ms-trondhjemites, and due to the impoverishment in CaO, these rocks lie on the albite/Kfeldspar-paragonite/muscovite line in the IAI vs. ASI diagram (Fig 5). Therefore, Qtz-Ms rocks are peraluminous, with ASI values considerably high due to the scarcity of feldspar (2.63-3.11; Fig. 5).

Trace elements

Ms-amphibolites

The general pattern of element distribution indicates important deviations from MORB composition, with enrichments in Ba, La, Pb, Sr, and Eu, and variable enrichment/depletion in Th and Zr (Fig. 7a), with homogeneous values from Sm to Ni (Fig. 7a).

The abundances of LREE and HREE range from 28 to 120 and from 12 to 25 the chondrite values, respectively (Fig. 8a). The chondrite-normalized REE diagrams are characterized by enriched LREE patterns showing basaltic affinity. The REE compositions of these Ms-amphibolites show different values to the Ms-lacking amphibolites from the mélange (Lázaro and García-Casco, 2008) indicating a heterogeneous subducting oceanic crust or a MOR-basaltic rock modified before, during, or after subduction. The (La/Yb)n ratio (normalized to chondrite, McDonough and Sun, 1995) varies from 2.1 to 5.1, showing fractionated patterns. The samples have no or positive Eu anomaly (Eu/Eu* = 0.98-1.45).

Ms-trondhjemites

The Ms-trondhjemites show fractionated patterns (Fig. 7b) similar to those of Ms-lacking trondhjemites of the Sierra del Convento mélange (grey field in Fig. 7b). Relative to the latter (Lázaro and García-Casco, 2008), the Ms-trondhjemites are enriched in Ba and Pb, depleted in Sr, and have similar contents in other element (Table 4, Fig. 7b).

LREE and HREE range from 3 to 24 and from 0.1 to 4.5 the chondrite values, respectively (Fig. 8b). The (La/Yb)n ratio ranges from 2 to 62, showing slightly to strongly fractionated patterns. The general low REE contents and (La/Yb)n ratios of the Ms-bearing trondhjemites can be explained in terms of a minor contribution of REE-bearing phases during melting of the amphibolites. The samples display positive Eu anomalies, with Eu/Eu* values higher than 1.1, reaching 10. This, in turn, suggests the important participation of plagioclase in the melting process, in agreement with the lack of peak plagioclase in the amphibolites (cf. García-Casco et al., 2008a).

The Nb–Y and Rb–(Y+Nb) diagrams (Fig. 9) of Pearce et al. (1984) indicates that the samples correspond to the volcanic arc setting, precluding ocean ridge, within-plate, and syn-collision settings. In these diagrams, adakites from a number of localities worldwide and Ms-lacking trondhjemites from the Sierra del Convento mélange compare well with the studied Ms-trondhjemitic rocks.

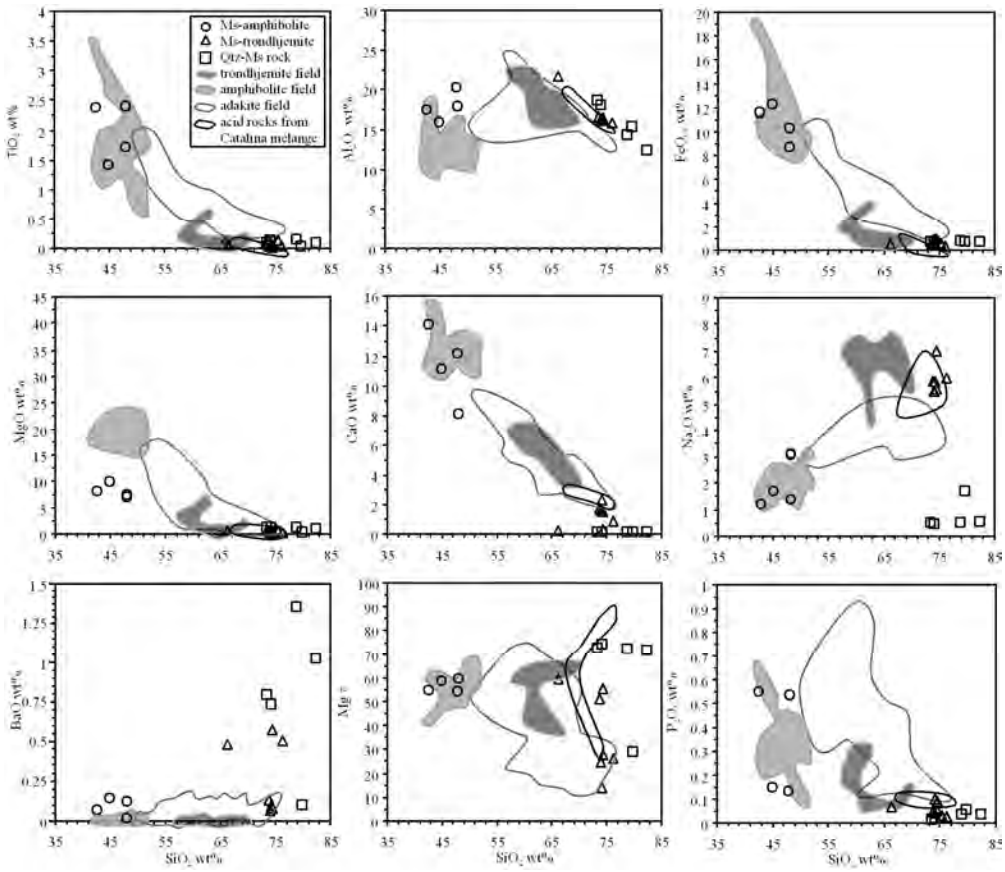

Fig. 4. Harker variation diagrams showing the composition of Ms-amphibolites, Ms-trondhjemites and Qtz-Ms rocks from the Sierra del Convento and, for comparison, N-MORB (Hofmann, 1988; Kelemen et al., 2003), altered MORB (Staudigel et al., 1996), amphibolites and trondhemites from the Sierra del Convento mélange (Lázaro and García-Casco, 2008), Cenozoic adakites (references as in Fig. 3), and acid rocks from the Catalina mélange, California (Sorensen and Grossman, 1989).

The Sr contents are high (from 86 to 410 ppm) and the Y contents are low (<10.7 ppm) (Table 4). This is clearly appreciated in the Sr/Y vs. Y diagram of Defant and Drummond (1990), where the Ms-trondhjemites mostly plot in the adakite field although they do not reach the high values of Ms-lacking trondhjemites of the mélange (Fig. 10a). However, in the (La/Yb)n vs. (Yb)n diagram (Martin, 1986) two different patterns can be observed; one group of Ms-trondhjemite samples plots outside the typical field of adakites, with low (La/Yb)n values (same as Ms-lacking trondhjemites from the Sierra del Convento and the acid rocks from the Catalina Schist mélanges), while other group of samples has distinctively higher (La/Yb)n values (Fig. 9b).

Qtz-Ms rocks

Given the mineral assemblage of these rocks, their geochemical characteristics are largely controlled by the chemistry of muscovite. They are slightly enriched in LILE compared to Ms-trondhjemites (Fig. 7c). Qtz-Ms rocks display fractionated chondrite-normalized REE patterns. The (La/Yb)n ratio ranges from 4 to 25 (except

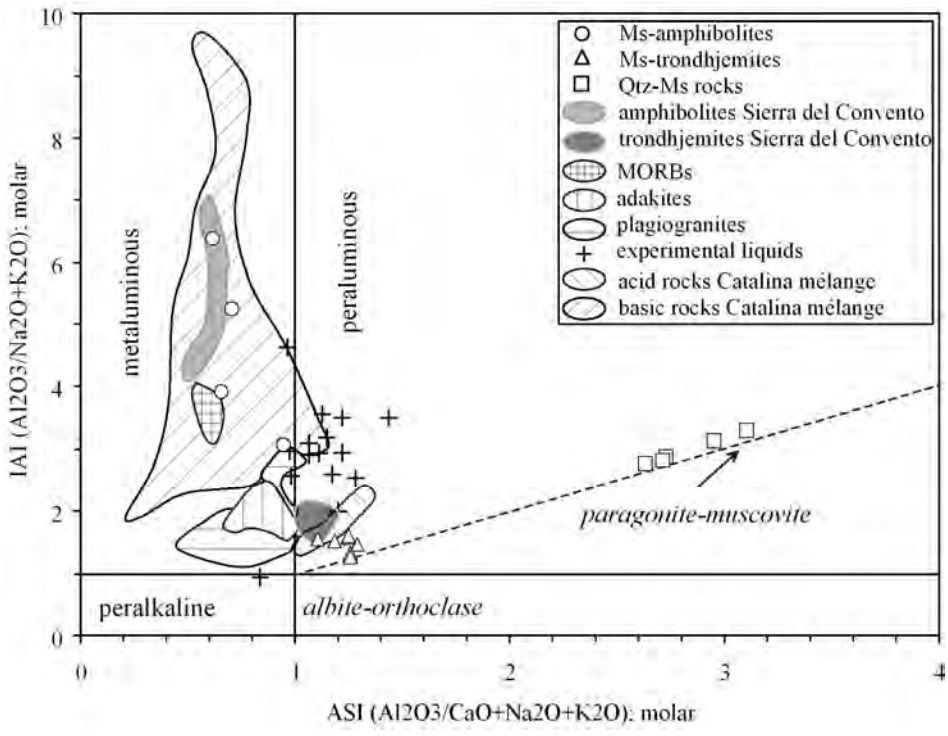

Fig. 5. IAI (inverse agpaitic index)-ASI (alumina saturation index) diagram with indication of the projection of alkali-feldspar and white micas for reference.

sample CV278a-I due to the presence of garnet, see Fig 2d) and the Eu anomaly is in general positive (Eu/Eu* = 1.8-3.5). These rocks present LREE values similar to the most enriched samples of Ms-trondhjemite, while their HREE values are similar to the medium HREE Ms-trondhjemite samples. The REE patterns for Qtz-Ms rocks are more fractionated than those of Ms-trondhjemites, as can be also appreciated from their larger (La/Yb)n ratios (Fig. 10b).

The Sr (<187 ppm) and Y contents are low (<5.4 ppm, in general) and similar to Ms-trondhjemites (Table 4). However, this rock type has very low Sr/Y, (La/Yb)n and (Yb)n (Figs. 9a and b).

Sr and Nd isotopes

The measured $^{87}Sr/^{86}Sr$ ratio of Ms-amphibolites ranges from 0.703745 to 0.705905, similarly to the isotopic ratio of the analyzed Ms-trondhjemite (0.705817). The measured $^{87}Sr/^{86}Sr$ ratios of Qtz-Ms rocks are higher (0.706729 and 0.708927). Values measured of 143Nd/144Nd range from 0.5122921 to 0.512997 (Ms-amphibolites), 0.512745 (Ms-trondhjemite) and 0.512550 and 0.512709 (Qtz-Ms rocks).

Following Lázaro and García-Casco (2008) and Lázaro et al. (2009) all isotopic measured data were corrected at 114 Ma (Table 3, Fig. 11). This age was established by SHRIMP zircon ages of trondhjemites of the Sierra del Convento mélange (Lázaro et al., 2009). The εNd(114 Ma) value of the analyzed Ms-trondhjemite (+1.94) deviates from that depleted mantle rocks and points to significant input of a

Table 2. Major (wt%) element (ppm) composition of Ms-amphibolites, Ms-trondhjemites, Ms-pegmatites and Average trondhjemite from the Sierra del Convento mélange.

Rock	Ms-amphibolites				Ms-trondhjemites							Qtz-Ms rocks				
Sample	CV139a	CV140a	CV230c	CV230a	CV201a	CV201g	SC-20	CV201h	CV230e	CU-72-I	CU-72	CV201d	CV201f	CV278a-I	CV53e-I	CV53e-II
SiO_2	46.27	46.54	42.08	44.24	75.55	73.80	73.09	65.63	72.72	73.37	73.18	81.15	77.11	77.90	71.47	71.82
TiO_2	1.66	2.31	2.34	1.39	0.03	0.05	0.04	0.06	0.07	0.02	0.03	0.08	0.13	0.02	0.08	0.12
$Al2O_3$	17.54	19.69	17.34	15.78	15.69	16.40	15.99	21.47	16.37	15.94	16.22	12.31	14.12	15.12	18.26	17.58
Fe_2O_{3tot}	11.11	9.39	12.75	13.45	0.28	0.40	0.61	0.51	0.59	0.98	1.03	0.73	0.84	0.76	0.78	0.72
MnO	0.21	0.22	0.19	0.11	0.03	0.05	0.04	0.01	0.01	0.04	0.03	0.01	0.01	0.29	0.02	0.01
MgO	6.71	7.08	7.90	9.70	0.05	0.25	0.05	0.38	0.31	0.19	0.17	0.93	1.11	0.16	1.05	1.06
CaO	11.84	7.95	13.99	11.01	0.87	0.34	2.28	0.21	1.73	1.49	1.60	0.14	0.15	0.17	0.19	0.16
Na_2O	1.32	3.02	1.21	1.65	5.93	6.92	5.74	9.01	5.77	5.50	5.40	0.54	0.48	1.66	0.48	0.43
K_2O	1.08	1.33	0.67	1.21	0.77	0.95	0.78	1.74	1.08	0.97	1.12	2.80	3.98	1.69	5.14	5.07
P_2O_5	0.13	0.52	0.54	0.15	0.03	0.05	0.04	0.07	0.05	0.09	0.10	0.03	0.03	0.06	0.01	0.02
LOI	1.68	2.15	0.77	1.14	0.50	0.67	1.73	0.85	1.22	1.19	0.94	1.38	1.83	1.61	2.37	2.89
Total	99.55	100.20	99.79	99.83	99.73	99.88	100.38	99.94	99.92	99.78	99.82	100.10	99.79	99.43	99.85	99.88
Mg #	54.47	59.90	55.11	58.83	26.13	55.32	13.73	59.61	51.00	27.75	24.64	71.62	72.36	29.43	72.73	74.47

Table 3 Rb/Sr and Sm/Nd isotope data of Ms-amphibolites, Ms-trondhjemites and Qtz-Ms rocks from Sierra del Convento mélange.

Rock Type	Sample	Rb	Sr	$^{87}Rb/^{86}Sr$	$^{87}Sr/^{86}Sr$	±2σ	Sm	Nd	$^{147}Sm/^{144}Nd$	$^{143}Nd/^{144}Nd$	±2σ
Ms-amphibolite	CV139a	15.6	504	0.089244	0.705481	0.002	4.1	13.9	0.177980	0.512921	0.002
Ms-amphibolite	CV140a	19.2	458	0.121178	0.703745	0.006	5.2	22	0.141026	0.512931	0.002
Ms-amphibolite	CV230a	22	273	0.232118	0.705905	0.002	2.5	7.6	0.200739	0.512997	0.002
Ms-trondhjemite	CV201a	11.5	182	0.182579	0.705817	0.002	0.88	2.6	0.206801	0.512745	0.006
Qtz-Ms rock	CV278a	40	181	0.639976	0.706729	0.004	1.02	1.89	0.326092	0.512709	0.004
Qtz-Ms rock	CV53e	85	98	2.507765	0.708927	0.002	0.87	2.4	0.220551	0.512550	0.002

Table 4. Trace element (ppm) composition of Ms-amphibolites, Ms-trondhjemites and Ms-pegmatitesfrom the Sierra del Convento mélange

Rock	Ms-amphibolites				Ms-trondhjemites					Qtz-Ms rocks						
Sample	CV139a	CV140a	CV230c	CV230a	CV201a	CV201g	SC-20	CV201h	CV230e	CU-72-I	CU-72	CV201d	CV201f	CV278a-I	CV53e-I	CV53e-II
Zr	98.50	211.50	201.80	62.40	17.80	13.80	24.60	70.50	47.00	21.20	22.60	42.50	19.30	25.70	42.00	31.70
Li	7.42	49.43	7.44	9.99	0.42	2.51	0.00	4.62	0.64	1.06	0.64	6.94	6.31	2.68	4.72	4.62
Rb	15.83	20.07	10.41	22.01	12.25	16.06	15.10	30.91	20.40	15.73	15.08	57.49	78.80	40.82	88.00	85.29
Cs	0.17	0.43	0.11	0.17	0.10	0.23	0.63	0.16	0.30	0.00	0.02	0.30	0.45	1.18	0.32	0.33
Be	0.71	1.77	1.19	1.29	1.00	7.87	0.77	1.02	0.50	0.93	0.89	1.96	2.38	3.65	2.36	2.20
Sr	509.69	458.03	530.77	258.87	191.50	86.00	388.83	97.49	409.93	149.65	132.17	21.01	24.21	186.81	99.61	99.01
Ba	1021.76	157.03	573.85	1266.63	4459.62	5063.09	758.73	4220.04	1095.06	647.36	504.31	9039.87	11810.00	833.17	6882.23	6328.76
Sc	37.64	27.12	44.94	50.73	0.70	7.68	0.36	0.37	0.00	0.00	0.00	1.56	4.56	3.72	5.65	4.77
V	279.55	184.86	321.94	350.22	3.70	20.17	2.99	14.95	5.86	2.56	3.13	37.61	51.66	5.26	20.41	18.22
Cr	332.74	292.51	405.24	544.63	39.38	34.21	129.25	118.63	164.89	27.74	136.17	40.34	35.37	26.19	53.97	40.14
Co	48.80	48.48	53.25	62.69	36.36	28.99	0.00	0.99	0.87	29.17	118.30	45.31	36.91	22.95	25.44	30.84
Ni	77.65	191.56	146.38	154.25	2.77	3.81	1.33	12.91	18.69	0.00	10.92	13.36	18.43	1.66	23.00	18.83
Zn	108.58	72.76	146.41	159.39	7.30	3.52	20.49	12.40	9.18	22.52	19.25	18.92	21.80	29.09	8.00	7.94
Y	28.53	31.84	44.71	22.67	10.67	5.36	0.74	3.27	0.64	1.32	1.47	1.80	4.08	17.37	5.33	5.41
Nb	7.60	21.36	30.35	4.94	2.46	12.15	0.55	1.95	0.29	1.22	2.70	4.24	8.18	7.41	5.60	4.50
Ta	0.74	1.64	2.29	0.32	0.56	1.30	0.02	0.26	0.03	0.10	0.45	0.99	0.65	0.86	0.45	0.47
Hf	0.96	0.37	1.27	0.86	0.37	0.27	0.20	2.63	0.14	0.05	0.08	0.20	0.36	0.44	0.95	0.50
Tl	0.11	0.04	0.10	0.22	0.12	0.12	0.18	0.28	0.21	0.15	0.14	0.47	0.64	0.24	0.60	0.57
Pb	11.34	1.55	6.59	5.41	20.01	13.89	3.12	6.67	4.83	9.03	8.21	2.31	2.99	10.18	5.43	4.98
U	0.40	0.78	1.06	0.61	0.63	1.54	0.12	3.09	0.06	0.23	0.52	0.90	2.56	10.41	0.77	1.01
Th	0.63	3.12	3.25	0.84	0.93	1.57	0.22	2.55	0.04	0.27	0.46	1.55	6.44	2.33	4.30	3.57
La	8.34	21.75	28.06	6.60	3.13	1.31	0.77	1.80	0.72	4.18	5.74	3.72	10.70	1.26	2.96	3.19
Ce	19.80	47.58	54.27	12.79	4.38	2.43	1.13	2.60	0.54	9.04	12.01	4.50	15.05	2.56	5.83	6.05
Pr	3.05	5.55	7.06	1.92	0.65	0.35	0.18	0.34	0.10	1.25	1.64	0.74	2.14	0.45	0.65	0.68
Nd	14.18	22.68	30.26	8.66	2.56	1.63	0.72	1.37	0.38	4.99	6.86	2.58	8.41	2.23	2.79	2.77
Sm	4.39	5.42	7.36	2.61	0.95	0.58	0.17	0.50	0.09	1.25	1.59	0.66	1.95	0.99	0.79	0.76
Eu	2.15	1.71	2.89	1.35	0.63	0.40	0.09	1.13	0.32	0.51	0.51	0.72	1.08	0.23	0.65	0.65
Gd	4.86	5.23	7.21	3.09	1.32	0.81	0.16	0.56	0.10	0.89	1.17	0.60	1.81	1.72	0.83	0.99
Tb	0.85	0.90	1.25	0.57	0.23	0.14	0.03	0.09	0.02	0.10	0.10	0.08	0.23	0.36	0.13	0.15
Dy	5.16	5.53	7.80	4.03	1.53	0.88	0.16	0.58	0.10	0.30	0.30	0.37	1.06	2.53	0.89	0.94
Ho	1.11	1.15	1.63	0.88	0.29	0.17	0.03	0.11	0.02	0.03	0.04	0.06	0.16	0.58	0.18	0.18
Er	3.07	3.06	4.50	2.40	0.77	0.48	0.08	0.23	0.05	0.06	0.07	0.14	0.36	1.62	0.53	0.47
Tm	0.45	0.46	0.66	0.35	0.11	0.07	0.01	0.03	0.01	0.00	0.01	0.02	0.05	0.26	0.08	0.07
Yb	2.64	2.91	4.14	2.01	0.73	0.44	0.10	0.16	0.05	0.06	0.06	0.13	0.29	1.90	0.54	0.39
Lu	0.37	0.43	0.63	0.30	0.11	0.08	0.01	0.02	0.01	0.01	0.00	0.02	0.04	0.28	0.09	0.05

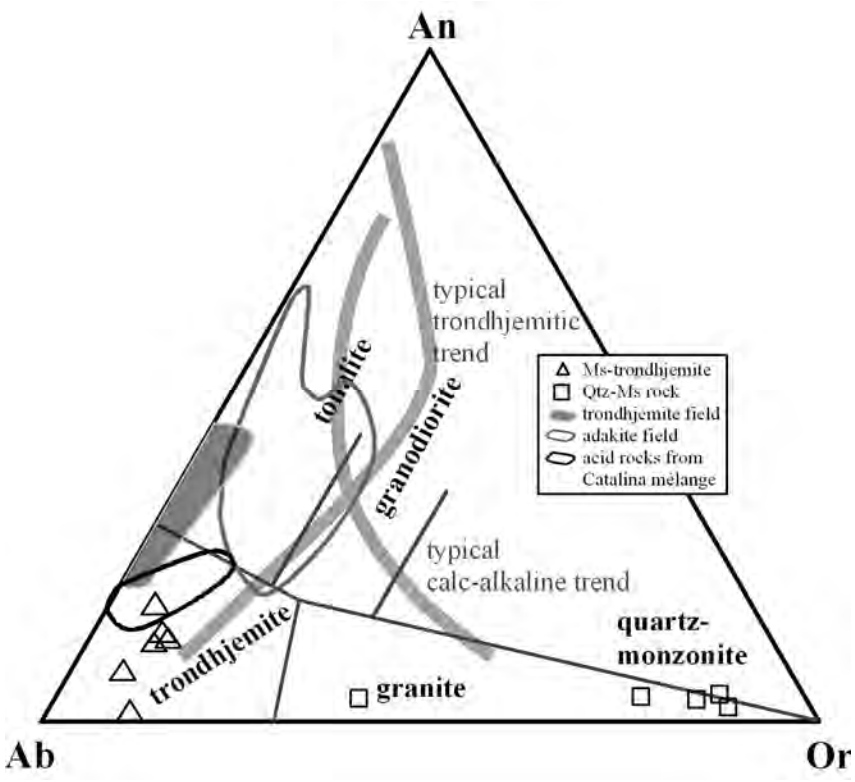

Fig. 6. Molecular normative (CIPW) diagram (O'Connor, 1965), with fields after Barker (1979) and typical calc-alkaline and trondhjemitic trends, of Ms-trondhjemites and Qtz-Ms rocks from Sierra del Convento mélange and, for comparison, K-poor trondhjemites from the Sierra del Convento, pegmatites and leucocratic segregates from the Californian Catalina Schist mélange (grey triangles) and Cenozoic adakites (sources as in Fig. 3).

continental crust/sediment component. The εNd (114 Ma) of Ms-amphibolites (from +5.8 to +6.9) do not overlap the Ms-trondhjemite value, and these rocks show the contribution of fluids derived from a sedimentary source to the oceanic crust component (i,e., Ms-lacking amphibolites; Lázaro and García-Casco, 2008). This indicates that the partial melting process involved fluid-present conditions, likely caused by the influx of external fluids into the amphibolites (García-Casco et al., 2008a), and that the external fluid had an isotopic composition typical of a source influenced by seawater or subducted (meta)sediments, as suggested by isotope composition of the Qtz-Ms rocks, the Atlantic Cretaceous Pelagic Sediment (AKPS, Jolly et al., 2006), which may be used as a proxy of potential subducted sediments, and sediment columns subducting at several trenches (Fig. 11).

In terms of Sr–Nd systematics, the Ms-trondhjemite is comparable to adakitic rocks from different localities. However, the Sr isotopic signature of the Ms-trondhjemite shows a significant sedimentary component in the origin of this type of rocks compared to adakites, which normally reflect a significant contribution of the mantle wedge in their isotopic signatures (Fig. 11). Moreover, both Ms-amphibolites and Ms-trondhjemites are also comparable to IAB field determined by Aleutians, Antilles, and Mariana Arcs rocks (GEOROC database http://georoc.mpch-

mainz.gwdg.de/georoc/Entry.html). This does not imply a common source and process of formation since the depleted source of adakites must be interpreted in terms of partial melting of MORB followed by interaction with a depleted supra-subduction mantle wedge. Notably, the Ms-trondhjemites studied here were trapped within their parental amphibolites and did not interact with the mantle wedge.

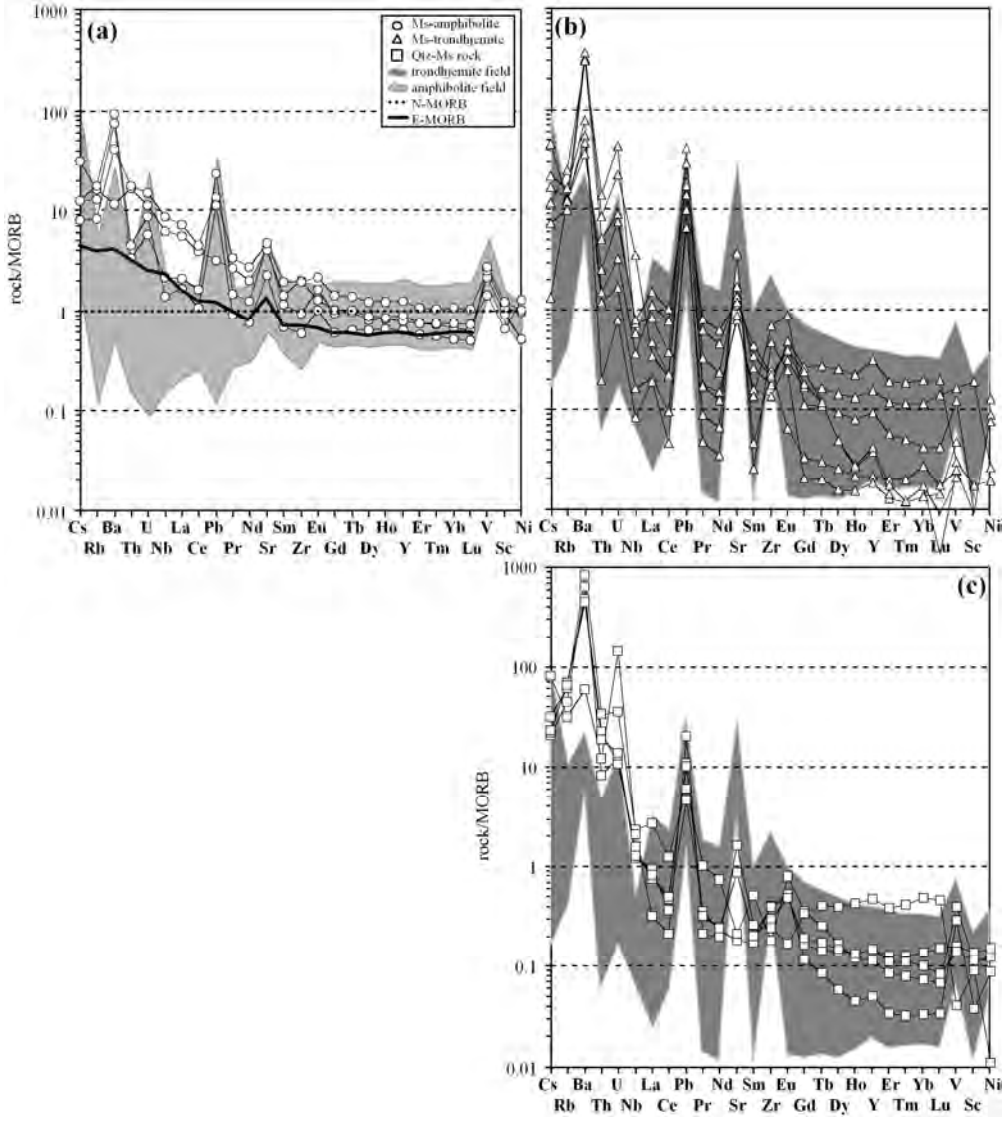

Fig. 7. N-MORB (Hofmann, 1988) normalized spider diagrams for: (a) Ms-amphibolites, (b) Ms-trondhjemites and (c) Qtz-Ms rocks from Sierra del Convento mélange. The fields of K-poor amphibolites and trondhjemites from the Sierra del Convento mélange (Lázaro and García-Casco, 2008) have been included for comparison.

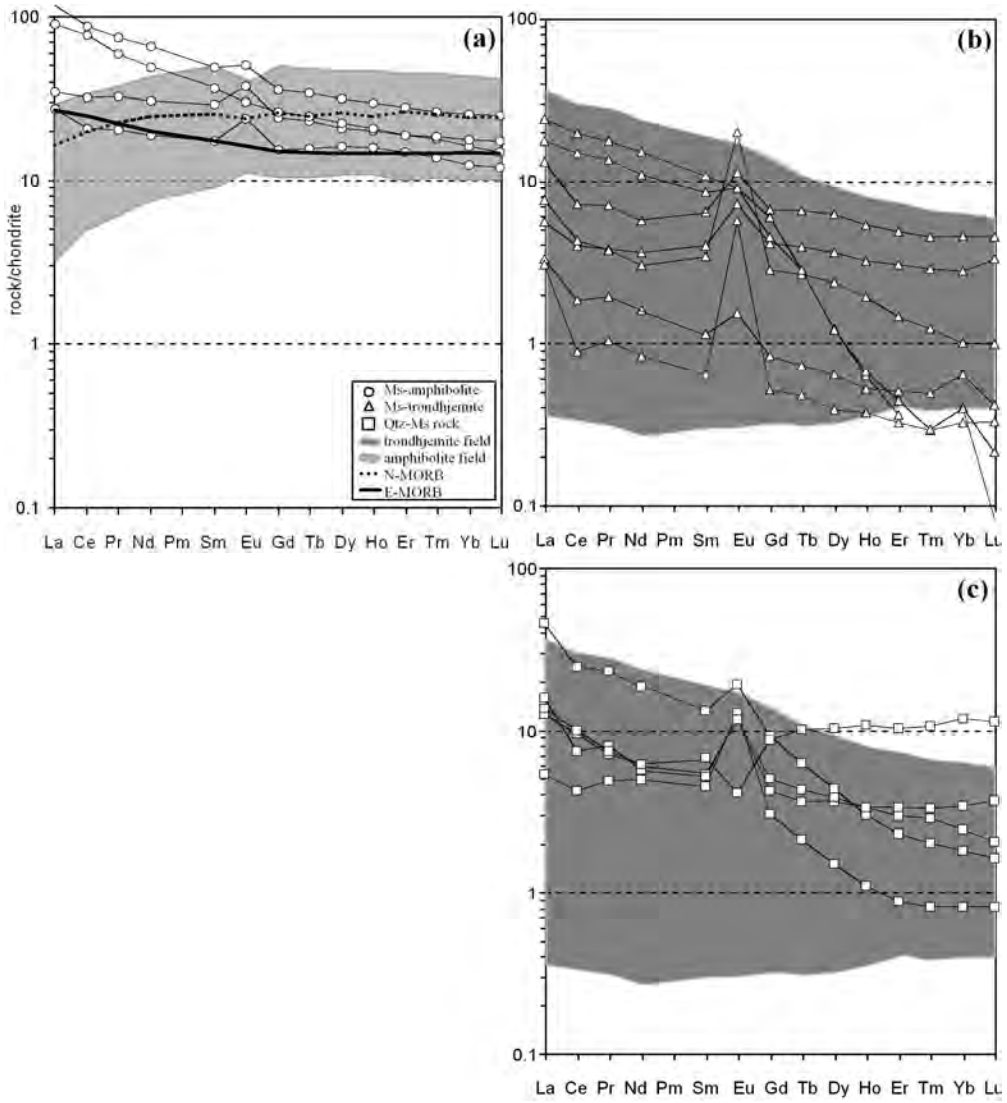

Fig. 8. Chondrite (McDonough and Sun, 1995) normalized REE patterns for: (a) Ms-amphibolites, (b) Ms-trondhjemites and (c) Qtz-Ms rocks from Sierra del Convento mélange. The fields of K-poor amphibolites and trondhjemites from the Sierra del Convento mélange (Lázaro and García-Casco, 2008) have been included for comparison.

DISCUSSION

The origin of Ms-protoliths

Lázaro and García-Casco (2008) demonstrated that the protoliths of the amphibolites from the Sierra del Convento mélange are basaltic rocks of N-MORB composition that evolved from a depleted mantle source, and did not identify LILE- and LREE-enriched island-arc, within-plate basalts and/or ocean plateau-like protoliths. These amphibolites are best explained as slightly modified residues of MORB protoliths, while the K-poor tonalites-trondhjemites constitute pristine slab melts formed during the initial stage of subduction of young oceanic crust.

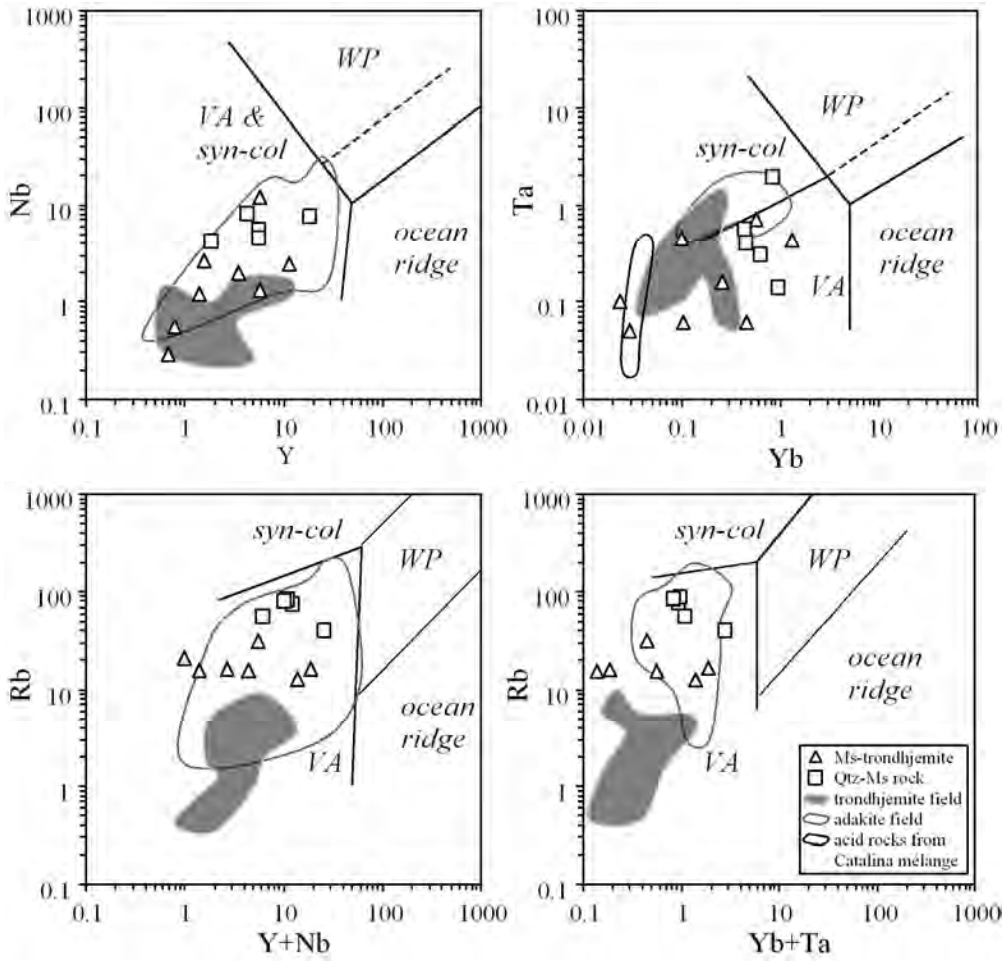

Fig. 9. Ms-trondhjemites and Qtz-Ms rocks plotted in discrimination diagrams for granitic rocks (Pearce et al., 1984) showing the fields of ocean ridge, volcanic arc (VA), syn-collisional, and within-plate (WP) granitic rocks. Grey fields correspond to trondhjemites from the Sierra del Convento mélange and white fields, to Cenozoic adakite compositions (references as in Fig. 3). Acid rocks from the Catalina mélange are plotted in the Ta-Yb diagram.

Petrological and geochemical resemblances can be established between the K-poor and Ms-bearing amphibolite blocks studied in this work. However, detailed petrological, elemental and isotopic geochemical data of the Ms-amphibolites indicate that these rocks suffered modifications before or during subduction/accretion involving the influence of seawater or sediment-derived fluids, respectively, that allowed the formation of muscovite and the concentration in K, Ba, La, U, and Pb. This fact can be observed in the isotopic signatures that appear modified by seawater influence or subducted sediment sources (Fig. 11).. In our view, the process perhaps involved seawater alteration of MORB at a sea-floor environment, but most of the geochemical characteristics of these rocks were acquired during high grade metamorphism and partial melting triggered by the infiltration of fluids derived from subducting sediments. This inference is based on

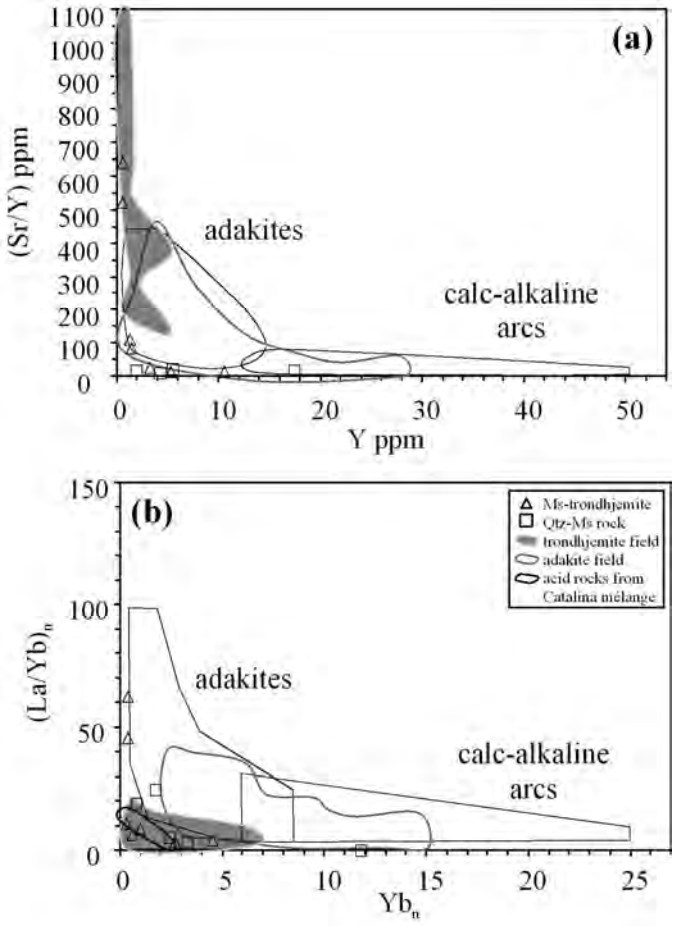

Fig. 10. Ms-trondhjemites and Qtz-Ms rocks plotted in (a) (Sr/Y) vs. Y and (b) $(La/Yb)_n$ vs. Yb_n diagrams with adakite and calc-alkaline arcs fields as defined by Defant and Drummond (1990) and Martin (1986), respectively. Grey fields correspond to K-poor trondhjemites from the Sierra del Convento mélange, and white fields to Cenozoic adakite compositions (references as in Fig. 3). Acid rocks from the Catalina mélange have been plotted in b).

the presence of Qtz+Ms rocks formed at depth after precipitation from a sediment-derived fluid and evidences provided by chemical zoning of muscovite (Blanco-Quintero et al., submitted).

The petrological and geochemical characteristics of the Ms-trondhjemites indicate a similar origin as that of the K-poor trondhjemites from the Sierra del Convento mélange. Field relations, petrological analysis, and elemental geochemistry allow us to infer that these rocks generated by partial melting of a Ms-bearing amphibolitic protolith or, most likely, a K-poor amphibolitic protolith invaded by a sediment-derived fluid enriched in LILE (Cs, Rb, Ba, U, and Pb). Conditions of melting were ca. 15 kbar and 750 °C (P-T conditions for sample CV139a; Lázaro et al., 2009). Isotopic data strengthen this view. The mixing curves between MORB and the isotopic composition of the sediment-derived fluid (i.e., Qtz+Ms rocks), explain the

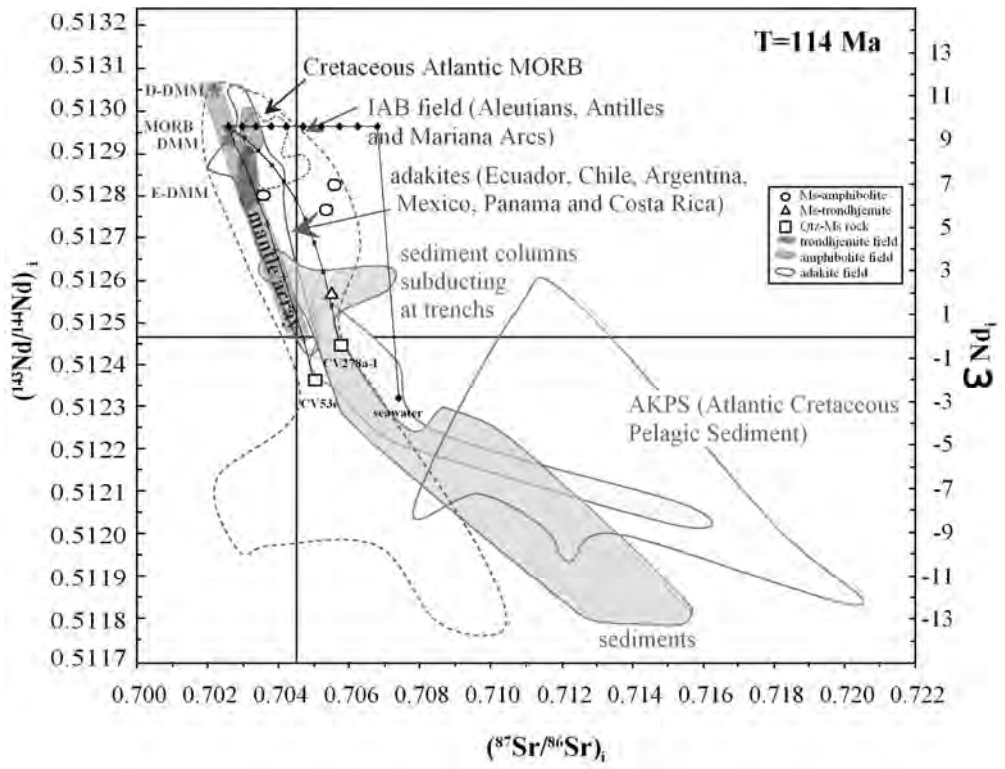

Fig. 11. $(^{87}Sr/^{86}Sr)_i$ vs. $(^{144}Nd/^{143}Nd)_i$ and εNd_i diagram. $\varepsilon Nd=((^{143}Nd/^{144}Nd_{sample}/^{143}Nd/^{144}Nd_{CHUR})-1)x10^4$, where CHUR=chondrite uniform reservoir (De Paolo, 1988). εNd and initial values calculated using $^{(143Nd/144Nd)}CHUR=0.512638$, $^{(147Sm/144Nd)}CHUR=0.1967$ (Wasserburg et al.,1981). Composition of seawater is from McCulloch et al. (1981) and Sm/Nd data is from Piepgras and Wasserburg (1980). Samples were corrected for T=114 Ma (see Lázaro et al., 2009). Data for depleted MORB mantle (DMM), depleted DMM (D-DMM), and enriched DMM (E-DMM) are from Workman and Hart (2005); N-MORB data are from Hart et al. (1999) and Kelemen et al. (2003); and Cretaceous Atlantic MORB data are from Jahn et al. (1980). The adakite field (grey colour line) includes data from Ecuador (Samaniego et al., 2005), Chile (Stern and Kilian, 1996), Argentina (Kay et al.,1993), Mexico (Aguillón-Robles et al., 2001), and Panama–Costa Rica (Defant et al., 1992); Marianas, Aleutians, and Antilles arc volcanic rocks field (dashed line), sediments and sediment columns subducting at trenches from the GEOROC database (http://georoc.mpch-mainz.gwdg.de/ georoc/Entry.html); and the Atlantic Cretaceous Pelagic Sediment (AKPS) field constructed after data from Jolly et al. (2006). Data from Ms-lacking amphibolites and trondhjemites from the Sierra del Convento (Lázaro and García-Casco, 2008) have been included. Mixing curves calculated between MORB and seawater and Qtz-Ms rocks are indicated.

distribution of Ms-bearing amphibolites and trondhjemites (Fig. 11). Similarly, the peraluminous character of the trondhjemites is best explained by infiltration of a peraluminous fluid during partial melting (Fig. 5).

Metasomatism and melting processes in subduction zones environments: melts in situ vs. melts in volcanic arcs

In arc magmas, elevated concentrations of large-ion-lithophile elements (LILE; e.g., Ba, K, Rb, Cs, Ca, Sr), U, and Pb relative to high-field-strength elements (e.g., Ti, Th, Hf, Nb, Zr) are considered key indicators of fluid addition to arc magma source regions. These fluids are released by dehydration of subducting altered MORB and

sediments of the slab. Transfer of LILE-, U-, and Pb-enriched fluids to the mantle wedge at sub-arc depths can trigger partial melting of peridotite and generate basaltic magmas with elevated Ba/Th, Sr/Th, Pb/Th, and U/Th, as well as radiogenic Sr (e.g., Breeding et al., 2004). However, these enriched fluids can also react with the subducted oceanic crust triggering partial melting upon appropriate conditions, forming melts derived from MORB source having a sedimentary imprint (e.g., Gao et al., 2007; Castro et al., 2010).

The experiments of Johnson and Plank (1999) in red clay at 700 ºC and 2.0 GPa allowed analyzing the type of sediment contribution from the subducting slab to the source of arc magmas and the magmas themselves. These authors determined that Rb, Sr, Ba and Pb are incompatible and Th is compatible below the solidus of metasediment. Hence, the addition of Th to arc magmas requires partial melting of the subducting sediment. The implied relations allow using the Ba/Th and Th/Nb ratios as monitors of effect of addition of fluids and melts derived from subducted sediment to arc magmas. Both Ms-amphibolites and Ms-trondhjemites have variable enrichment in Ba/Th and are poor in Th/Nb, suggesting the influence of sediment derived fluid (Fig. 12). The Qtz-Ms rocks have higher Th/Nd and relatively low Ba/Th ratio, suggesting a mixed component influence of a sediment-derived fluid and melt. The compositions of the Ms-trondhjemite and Qtz-Ms rocks indicate contrasted processes of sedimentary input in the subduction environment, though a

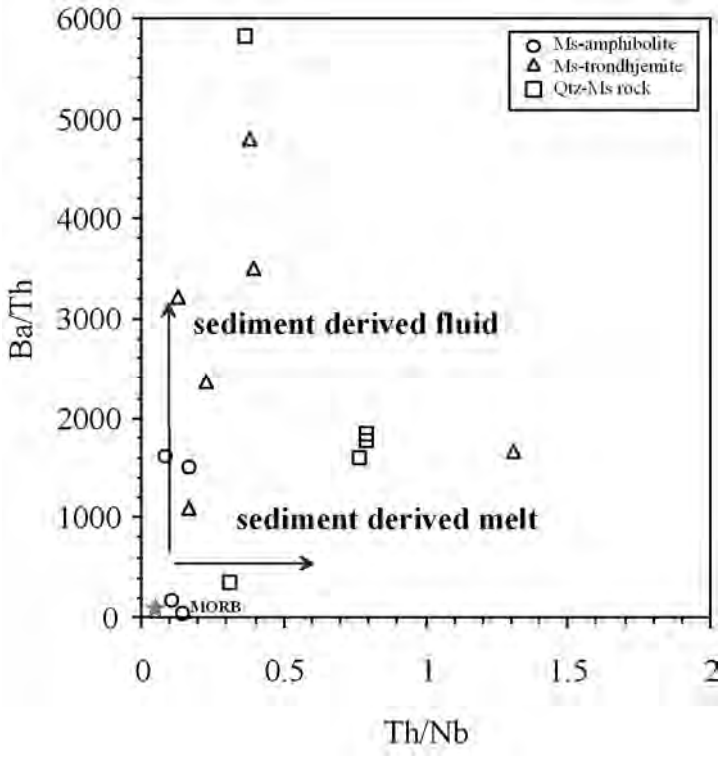

Fig. 12. Ba/Th versus Th/Nb of rocks showing the effect of addition of fluids and melts derived from subducted sediment to arc magmas (after Fretzdorff et al., 2002). N-MORB composition after Hoffman (1988).

sediment-derived fluid seems to be the agent that explains the formation of the studied trondhjemitic and Qtz-Ms rocks (cf. Fretzdorff et al. 2002); while the Qtz-Ms rocks may represent the result of the crystallization of this fluid or melt evolved from the sediments.

CONCLUSIONS

Major, trace element and isotopic compositions of the Ms-amphibolite from Sierra del Convento mélange indicate a MORB affinity altered by seawater and fluids evolved from subducted sediments. Fluid availability was the key controlling factor in the melting process. This process and the P-T conditions reached during subduction/acretion triggered partial melting and formation of K-rich trondhjemitic melt having an adakitic geochemical affinity. This melt did not escape and react with the upper plate peridotite, representing an end-member (pristine slab melts) of the volcanic arc series. The hydrothermal Qtz-Ms rocks have a strong sedimentary imprint, with the higher concentrations of mobile elements (K, Ba, etc.) and more evolved Sr-Nd isotopic composition. These rocks represent the crystallization products of fluids produced by dehydration of sedimentary source in the slab and involved in the partial melting process that generated the Ms-trondhjemitic melts.

ACKNOWLEDGMENTS

The authors thank financial support from Spanish MEC and MICINN projects CGL2006-08527/BTE and CGL2009-12446. This is a contribution to IGCP-546 “Subduction zones of the Caribbean”.

REFERENCES

Aguillón-Robles, A., Calmus, T., Benoit, M., Bellon, H., Maury, R.O., Cotten, J., Bourgois, J., Michaud, F., 2001. Late Miocene adakites and Nb-enriched basalts from Vizcaino Peninsula, Mexico: indicators of East Pacific Rise subduction below Southern Baja California? Geology 29 (6), 531–534.

Barker, F.,1979. Trondhjemite:definition, environment and hypotheses of origin. In: Barker, F. (Ed.), Trondhjemites, dacites and related rocks. Elsevier, Amsterdam, pp. 1–12.

Beate, B., Monzier, M., Spikings, R., Cotten, J., Silva, J., Bourdon, E., Eissen, J.P., 2001. Mio-Pliocene adakite generation related to flat subduction in southern Ecuador: the Quimsacocha volcanic center. Earth and Planetary Science Letters 192 (4), 561–570.

Bebout, G.E., Barton, M.D., 1993. Metasomatism during subduction — products and possible paths in the Catalina schist, California. Chemical Geology 108 (1–4), 61–92.

Bebout, G. E., Barton, M. D., 2002. Tectonic and metasomatic mixing in a subduction-zone melange: insights into the geochemical evolution of the slab-mantle interface, Chemical Geology 187, 79-106.

Bebout, G.E., 2007. Metamorphic chemical geodynamics of subduction zones. Earth and Planetary Science Letters 260, 373–393.

Benoit, M., Aguillón-Robles, A., Calmus, T., Maury, R.C., Bellon, H., Cotten, J., Bourgois, J., Michaud, F., 2002. Geochemical diversity of Late Miocene volcanism in southern Baja California, Mexico: implication of mantle and crustal sources during the opening of an asthenospheric window. Journal of Geology 110 (6), 627–648.

Blanco Quintero, I.F., 2003. Nuevos datos petroquímicos y petrográficos de las migmatitas y metamorfitas de algunos sectores del bloque oriental cubano (sectores Moa-Baracoa y Sierra del Convento). Master's Thesis, University of Moa, Moa (Cuba), 77 pp.

Blanco-Quintero, I.F., García-Casco, A., Rojas-Agramonte, Y., Rodríguez-Vega, A., Lázaro, C., Iturralde-Vinent, M.A., 2010a. Metamorphic evolution of subducted hot oceanic crust, La Corea mélange, Cuba. American Journal of Science (in press).

Blanco-Quintero, I.F., Proenza, J.A., García-Casco, A., Tauler, E., Galí, S., 2010b. Serpentinites and serpentinites within a fossil subdution channel: La Corea melange, eastern Cuba. Geologica Acta (in press).

Boiteau, A., Saliot, P., Michard, A., 1972. High-pressure metamorphism in ophiolite complex of purial (Oriente, Cuba). Comptes Rendus Hebdomadaires Des Seances De L Academie Des Sciences Serie D 274 (15), 2137–2140.

Bourdon, E., Eissen, J.P., Gutscher, M.A., Monzier, M., Samaniego, P., Robin, C., Bollinger, C., Cotten, J., 2002. Slab melting and slab melt metasomatism in the Northern Andean Volcanic Zone: adakites and high-Mg andesites from Pichincha volcano (Ecuador). Bulletin De La Societe Geologique De France 173 (3), 195–206.

Bourdon, E., Eissen, J.P., Gutscher, M.A., Monzier, M., Hall, M.L., Cotten, J., 2003. Magmatic response to early aseismic ridge subduction: the Ecuadorian margin case (South America). Earth and Planetary Science Letters 205 (3–4), 123–138.

Breeding, C.M., Ague, J.J., Bröcker, M., 2004. Fluid-metasedimentary rock interactions in subduction-zone melange: Implications for the chemical composition of arc magmas. Geology 32, 1041–1044.

Castro, A., Gerya, T., García-Casco, A., Fernández, C., Díaz-Alvarado, J., Moreno-Ventas, I., Löw, I., 2010. Melting Relations of MORB–Sediment Mélanges in Underplated Mantle Wedge Plumes; Implications for the Origin of Cordilleran-type Batholiths. Journal of Petrology 51, 1267-1295.

Castro, A., Gerya, T.V., 2008. Magmatic implications of mantle wedge plumes: Experimental study. Lithos 103 (1-2), 138-148.

Cobiella, J., Quintas, F., Campos, M., Hernández, M., 1984. Geología de la Región Central y Suroriental de la Provincia de Guantánamo. Editorial Oriente, Santiago de Cuba, Santiago de Cuba, 125 p.

Defant, M.J., Drummond, M.S., 1990. Derivation of some modern arc magmas by melting of young subducted lithosphere. Nature 347 (6294), 662–665.

Defant, M.J., Jackson, T.E., Drummond, M.S., Deboer, J.Z., Bellon, H., Feigenson, M.D., Maury, R.C., Stewart, R.H., 1992. The geochemistry of young volcanism throughout Western Panama and Southeastern Costa-Rica—an overview. Journal of the Geological Society 149, 569–579.

Fretzdorff, S., Livermore, R. A., Devey, C. W., Leat, P. T., Stoffers, P., 2002. Petrogenesis of the back-arc East Scotia Ridge, South Atlantic Ocean. Journal of Petrology, 43, 1435– 1467.

Gao, Y., Hou, Z., Kamber, B.S., Wei, R., Meng, X., Zhao, R., 2007. Adakite-like porphyries from the southern Tibetan continental collision zones: evidence for slab melt metasomatism. Contributions to Mineralogy and Petrology 153, 105–120.

García-Casco, A., Torres-Roldán, R.L., Iturralde-Vinent, M.A., Millán, G., Núñez Cambra, K., Lázaro, C., Rodríguez Vega, A., 2006. High pressure metamorphism of ophiolites in Cuba. Geologica Acta 4, 63–88.

García-Casco, A., Lázaro, C., Rojas-Agramonte, Y., Kröner, A., Torres-Roldán, R.L., Núñez, K., Millán, G., Neubauer, F., Blanco-Quintero, I., 2008a. Partial melting and counterclockwise P-T path of subducted oceanic crust (Sierra del Convento mélange, Cuba). Journal of Petrology 49, 128–161.

García-Casco, A., Iturralde-Vinent, M. A., Pindell, J., 2008b. Latest Cretaceous collision ⁄ accretion between the Caribbean Plate and Caribeana: origin of metamorphic terranes in the Greater Antilles. International Geology Review 50, 781– 809.

Gerya, T. V., Yuen, D. A., 2003. Rayleigh–Taylor instabilities from hydration and melting propel 'cold plumes' at subduction zones. Earth and Planetary Science Letters 212 (1-2), 47-62.

Gill, J.B., 1981. Orogenic Andesites and Plate Tectonics. Springer-Verlag, Berlin. 390 pp.

Gorczyk, W., Gerya, T.V., Connolly, J.A.D., Yuen, D.A., 2007. Growth and mixing dynamics of mantle wedge plumes. Geology 35, 587–590.

Govindaraju, K., 1994. Compilation of working values and sample description for 383 geostandards. Geostandards Newsletter 18, 1–158.

Grove, M., Bebout, G.E., 1995. Cretaceous tectonic evolution of coastal southern California: insights from the Catalina Schist. Tectonics 14 (6), 1290–1308.

Gyarmati, P., Méndez, I., Lay, M., 1997. Caracterización de las rocas del arco de islas Cretácico en la Zona Estructuro-Facial Nipe-Cristal-Baracoa. In: Furrazola, G.F., Núñez-Cambra K.E., eds., Estudios sobre Geología de Cuba, Ciudad de la Habana, Instituto de Geología y Paleontología, 357-364.

Hart, S.R., Blusztajn, J., Dick, H.J.B., Meyer, P.S., Muehlenbachs, K.,1999. The fingerprint of seawater circulation in a 500-meter section of ocean crust gabbros. Geochimica Et Cosmochimica Acta 63 (23–24), 4059–4080.

Hernández, M., Canedo, Z., 1995. Geoquímica de las ofiolitas meridionales de Cuba oriental. Minería y Geología 3, 3–9.

Hofmann, A.W., 1988. Chemical differentiation of the Earth — the relationship between mantle, continental-crust, and oceanic-crust. Earth and Planetary Science Letters 90 (3), 297–314.

Iturralde-Vinent, M.A., 1998. Sinopsis de la Constitución Geológica de Cuba. Acta Geológica Hispánica 33, 9–56.

Iturralde-Vinent, M. A., Millán, G., Korkas, L., Nagy, E., Palón, J., 1996. Geological interpretation of the Cuban K-Ar data base. In: Ofiolitas Y Arcos Volcánicos de Cuba (ed. Iturralde-Vinent, M. A.), pp. 48–69, IGCP Project 364, Miami, FL.

Iturralde-Vinent, M. A., Díaz Otero, C., Rodríguez Vega, A., Díaz Martínez, R., 2006. Tectonic implications of paleontologic dating of Cretaceous-Danian sections of Eastern Cuba. Geologica Acta, 4, 89–102.

Jahn, B.M., Bernardgriffiths, J., Charlot, R., Cornichet, J., Vidal, F., 1980. Nd and Sr isotopic compositions and REE abundances of cretaceous MORB (Holes 417d and 418a, Legs 51, 52 and 53). Earth and Planetary Science Letters 48 (1), 171–184.

Johnson, M.C., Plank, T., 1999. Dehydration and melting experiments constrain the fate of subducted sediments: Geochemistry Geophysics and Geosystems 1, p. 1999GC000014.

Jolly, W.T., Lidiak, E.G., Dickin, A.P., 2006. Cretaceous to mid-Eocene pelagic sediment budget in Puerto Rico and the Virgin Islands (northeast Antilles Island arc). Geologica Acta 4 (1–2), 35–62.

Kay, S.M., Ramos, V.A., Marquez, M., 1993. Evidence in Cerro-Pampa volcanic-rocks for slab-melting prior to ridge-trench collision in southern South-America. Journal of Geology 101 (6), 703–714.

Kelemen, P.B., Hanghøj, K., Green, A.R., 2003. One viewof the geochemistry of subductionrelated magmatic arcs, with an emphasis on primitive andesite and lower crust. In: Rudnick, R. (Ed.), Geochemistry of the Crust: Treatise of Geochemistry. Elsevier, Amsterdam, pp. 593–659.

Kretz, R., 1983. Symbols for rock-forming minerals. American Mineralogist, 68, 277–279.

Kulachkov, L.V., Leyva, R.C., 1990. Informe sobre los resultados de los trabajos de reconocimiento geolo´gico para cuarzo filoniano en la parte oriental de Cuba. Instituto Superior Minero-Metalúrgico, Moa, Cuba.

Kushiro, I., 1990. Partial melting of mantle wedge and evolution of island-arc crust. Journal of Geophysical Research-Solid Earth and Planets 95 (B10), 15929–15939.

Lázaro, C., García-Casco, A., 2008. Geochemical and Sr-Nd isotope signatures of pristine slab melts and their residues (Sierra del Convento mélange, eastern Cuba). Chemical Geology 255:120–133.

Lázaro, C., García-Casco, A., Neubauer, F., Rojas-Agramonte, Y., Kröner, A., Iturralde-Vinent, M.A., 2009. Fifty five-million-year history of oceanic subduction and exhumation in the northern edge of the Caribbean plate (Sierra del Convento mélange, Cuba). Journal of Metamorphic Geology, 27, 19-40.

Le Maitre, R.W., Bateman, P., Dudek, A., Keller, J., Lameyre Le Bas, M.J., Sabine, P.A., Schmid, R., Sorensen, H., Streckeisen, A., Woolley, A.R., Zanettin, B., 1989. A Classification of Igneous Rocks and Glossary of Terms. Blackwell, Oxford. 196 pp.

Leyva, R. C., 1996. Características geológicas, regularidades de distribución y perspectivas de utilización del cuarzo filoniano de la región oriental de Cuba. Masters Thesis, University of Moa, Moa, Cuba.

Marchesi, C., Garrido, C.J., Godard, M., Proenza, J.A., Gervilla, F., Blanco-Moreno, J., 2006. Petrogenesis of highly depleted peridotites and gabbroic rocks from the Mayarí-Baracoa Ophiolitic Belt (eastern Cuba). Contributions to Mineralogy and Petrology 151 (6), 717–736.

Marchesi, C., Garrido, C. J., Bosch, D., Proenza, J. A., Gervilla, F., Monié, P., Rodríguez-Vega, A., 2007. Geochemistry of Cretaceous magmatism in eastern Cuba: recycling of North American continental sediments and implications for subduction polarity in the Greater Antilles Paleo-arc. Journal of Petrology 48, 1813-1840.

Martin, H., 1986. Effect of steeper Archaean geothermal gradient on geochemistry of subduction-zone magmas. Geology 14, 753–756.

Martin, H., 1999. The adakitic magmas: modern analogues of Archaean granitoids. Lithos 46 (3), 411–429.

McCulloch, M.T., Gregory, R.T., Wasserburg, G.J., Taylor, H.P., 1981. Sm–Nd, Rb–Sr, and O18–O16 isotopic systematics in an oceanic crustal section — evidence from the Samail Ophiolite. Journal of Geophysical Research 86 (NB4), 2721–2735.

McDonough, W.F., Sun, S.S., 1995. The composition of the Earth. Chemical Geology 120 (3–4), 223–253.

Millán, G., 1996. Metamorfitas de la asociación ofiolítica de Cuba. In: Iturralde- Vinent, M.A. (Ed.), Ofiolitas y Arcos Volcanicos de Cuba. IGCP Project 364, Miami (USA), pp. 147–153.

Millán, G., Somin, M., 1985. Nuevos aspectos sobre de la estratigrafía del macizo metamórfico de Escambray. Contribución al conocimiento geológico de las metamorfitas del Escambray y Purial. Instituto de Gelogía y Paleontología, La Habana.

Morris, P.A., 1995. Slab melting as an explanation of quaternary volcanism and aseismicity in southwest Japan. Geology 23 (5), 395–398.

O'Connor, J.T., 1965. A classification of quartz-rich igneous rocks based on feldspar ratios. 525B. Professional Paper. U. S. Geological Survey. B79–B84 pp.

Pearce, J.A., Harris, N.B.W., Tindle, A.G., 1984. Trace-element discrimination diagrams for the tectonic interpretation of granitic-rocks. Journal of Petrology 25 (4), 956–983.

Peccerillo, A., Taylor, S.R., 1976. Geochemistry of Eocene calc-alkaline volcanic-rocks from Kastamonu Area, Northern Turkey. Contributions to Mineralogy and Petrology 58 (1), 63–81.

Piepgras, D.J.,Wasserburg, G.J., 1980. Neodymium isotopic variations in seawater. Earth and Planetary Science Letters 50 (1), 128–138.

Proenza, J. A., Díaz-Martínez, R., Iriondo, A., Marchesi, C., Melgarejo, J.C., Gervilla, F., Garrido, C.J., Rodríguez-Vega, A., Lozano-Santacruz, R., Blanco-Moreno, J.A., 2006. Primitive Cretaceous island-arc volcanic rocks in eastern Cuba: the Téneme Formation. Geologica Acta 4, 103–121.

Rapp, R. P., Shimizu, N., Norman, M. D., Applegate, G. S., 1999. Reaction between slab-derived melts and peridotite in the mantle wedge: experimental constraints at 3.8 Gpa. Chemical Geology 160 (4), 335-356

Sajona, F.G., Maury, R.C., Bellon, H., Cotten, J., Defant, M., 1996. High field strength element enrichment of Pliocene–Pleistocene Island arc basalts, Zamboanga Peninsula, western Mindanao (Philippines). Journal of Petrology 37 (3), 693–726.

Sajona, F.G., Maury, R.C., Pubellier, M., Leterrier, J., Bellon, H., Cotten, J., 2000. Magmatic source enrichment by slab-derived melts in a young post-collision setting, central Mindanao (Philippines). Lithos 54 (3–4), 173–206.

Samaniego, P., Martin, H., Monzier, M., Robin, C., Fornari, M., Eissen, J.P., Cotten, J., 2005. Temporal evolution of magmatism in the Northern Volcanic Zone of the Andes: the geology and petrology of Cayambe Volcanic Complex (Ecuador). Journal of Petrology 46 (11), 2225–2252.

Smith, D.R., Leeman, W.P., 1987. Petrogenesis of Mount St-Helens dacitic magmas. Journal of Geophysical Research-Solid Earth and Planets 92 (B10), 10313–10334.

Smithies, R.H., 2000. The Archaean tonalite-trondhjemite-granodiorite (TTG) series is not an analogue of Cenozoic adakite. Earth and Planetary Science Letters 182 (1), 115–125.

Somin, M., Millán, G., 1981. Geology of the Metamorphic Complexes of Cuba (in Russian). Nauka, Moscow. 219 pp.

Somin, M.L., Arakelyants, M.M., and Kolesnikov, E. M., 1992. Age and tectonic significance of high-pressure metamorphic rocks in Cuba. International Geology Review 34, 105–118.

Sorensen, S.S., 1988. Petrology of amphibolite-facies mafic and ultramafic rocks from the Catalina Schist, Southern-California — metasomatism and migmatization in a subduction zonemetamorphic setting. Journal of Metamorphic Geology 6 (4), 405–435.

Sorensen, S.S., Grossman, J.N., 1989. Enrichment of trace-elements in garnet amphibolites from a paleo-subduction zone — Catalina Schist, Southern-California. Geochimica Et Cosmochimica Acta 53 (12), 3155–3177.

Sorensen, S.S., Barton, M.D., 1987. Metasomatism and partial melting in a subduction complex: Catalina Schist, southern California. Geology 15, 115-118.

Staudigel, H., Plank, T., White, W.M., Schmincke, H., 1996. Geochemical fluxes during seafloor alteration of the basaltic upper oceanic crust: DSDP Sites 417 and 418. In: Bebout, G.E., Scholl, S.W., Kirby, S.H., Platt, J.P. (Eds.), Subduction from Top to Bottom. American Geophysical Union, Washington, DC, pp. 19–38.

Stern, C.R., Kilian, R., 1996. Role of the subducted slab, mantle wedge and continental crust in the generation of adakites from the Andean Austral volcanic zone. Contributions to Mineralogy and Petrology 123 (3), 263–281.

Tatsumi, Y., Kogiso, T., 1997. Trace element transport during dehydration processes in the subducted oceanic crust .2. Origin of chemical and physical characteristics in arc magmatism. Earth and Planetary Science Letters 148 (1–2), 207–221

Wasserburg, G.J., Jacobsen, S.B., DePaolo, D.J., McCulloch, M.T., Wen, T., 1981. Precise determination of Sm/Nd ratios, Sm and Nd isotopic abundances in standard solutions. Geochimica Et Cosmochimica Acta 45, 2311–2323.

Workman, R.K., Hart, S.R., 2005. Major and trace element composition of the depleted MORB mantle (DMM). Earth and Planetary Science Letters 231 (1–2), 53–72.

Yogodzinski, G.M., Kay, R.W., Volynets, O.N., Koloskov, A.V., Kay, S.M., 1995. Magnesian Andesite in the Western Aleutian Komandorsky Region — implications for slab melting and processes in the mantle wedge. Geological Society of America Bulletin 107 (5), 505–519.